First-principles description of atomic gold chains on Ge(001)

S. López-Moreno,[1] A. H. Romero,[1] A. Muñoz,[2] and U. Schwingenschlögl[3,*]

[1]*CINVESTAV–Queretaro, Libramiento Norponiente No. 2000, Real de Juriquilla, 76230 Queretaro, Mexico*
[2]*MALTA Consolider Team, Departamento de Física Fundamental II, Instituto de Materiales y Nanotecnología,*
Universidad de La Laguna, La Laguna 38205, Tenerife, Spain
[3]*PSE Division, KAUST, Thuwal 23955-6900, Saudi Arabia*

We have performed density-functional theory calculations, including the spin-orbit correction, to investigate atomic gold chains on Ge(001). A set of 26 possible configurations of the Au/Ge(001) system with $c(4 \times 2)$ and $c(8 \times 2)$ symmetries is studied. Our data show that the $c(4 \times 2)$ order results in the lowest energy, which is not in direct agreement with recent experiments. Using total-energy calculations, we are able to explain these differences. We address the electronic band structure and apply the Tersoff-Hamann approach to correlate our data to scanning-tunneling microscopy (STM). We obtain two highly competitive structures of the atomic Au chains for which we report simulated STM images in order to clarify the composition of the experimental Au/Ge(001) surface.

Having been investigated steadily since decades, semiconductor surfaces are recently attracting new attention due to a great capacity of hosting monatomic metallic chains. While mechanical fabrication by scanning-tunneling microscopy (STM) tip techniques[1,2] or break junction techniques[3,4] is limited to a chain length of several ten atoms, utilization of self-organization processes of adatoms on surfaces can lead to much longer chains. These chains are of great interest both for basic research and for various applications because they give rise to a (quasi-) one-dimensional electron system. In this context, Schäfer *et al.*[5] recently discovered a new system: self-organized atomic Au chains on Ge(001) with a $c(8 \times 2)$ long-range order. These Au nanowires appear to be largely decoupled from the Ge substrate and therefore have been put forward as a model system for a Luttinger liquid.[6–8]

Self-organized In wires on Si(111) (Ref. 9) and Au wires on Si(533),[10] on the contrary, have been found to exhibit a significant coupling to the substrate. For the Ge(001) surface, Au growth, in general, comes along with a large variety of ordering phenomena as a function of both coverage and growth temperature.[11] The Ge(001) surface thereby is subject to a strong relaxation. In particular, a missing-row reconstruction with emerging microfacets of the Ge(111) type,[12] which is known from the clean Au(110), Ir(110), and Pt(110) surfaces,[13,14] has been reported. Adsorption of Pt atoms on Ge(001) results in highly ordered arrays of nanowires, which show very little defects and reach lengths of several 100 nm.[15,16] The latter system has been investigated in detail[17,18] by *ab initio* calculations based on the density-functional theory (DFT),[19] demonstrating the capacity of *ab initio* methods for interpreting experimental data, particularly, from STM and angular-resolved photoelectron spectroscopy. Specifically, the pseudopotential method provides useful information by accurate theoretical STM images, which help to understand experimental data.[20]

Our findings are based on total-energy DFT calculations in the framework of the projector-augmented wave method,[21,22] using the Vienna *ab initio* simulation package.[23,24] For the exchange-correlation functional, we apply the generalized gradient approximation and the Perdew-Burke-Ernzerhof scheme.[25] All our data have been obtained under the inclusion of the spin-orbit coupling, which is essential for describing the electronic as well as optical properties of Au systems.[26] We use a 250-eV-plane-wave energy cutoff and have carefully checked the convergence of our calculations. The Monkhorst scheme is employed for Brillouin-zone integrations,[27] applying meshes of $10 \times 10 \times 10$ and $8 \times 4 \times 1$ points in the bulk and the surface calculation, respectively. Our structure optimization leads to residual forces of less than 0.01 eV/Å (for each Cartesian direction).

Our calculations provide key results on the behavior of self-assembled Au atoms on a Ge(001) surface and on the question of how the ordering is affected by the presence of the substrate. The interaction is not only due to electron transfer but is also determined by a reconstruction on an atomic scale, which draws adatoms into the surface.

A good overview of the experimental and theoretical efforts to resolve the surface reconstruction of the clean Ge(001) surface can be obtained from Refs. 28 and 29. It has been established that neighboring Ge surface atoms form asymmetric dimers in order to saturate one dangling bond, whereas the relaxation of the bulk is rather small. The dimers line up to characteristic dimer rows. Moreover, the lattice is further stabilized by a distinct buckling pattern of the surface dimers, which leads to a $c(4 \times 2)$ superstructure at low temperatures. DFT-based structure optimization has fully reproduced x-ray diffraction data for the clean Ge(001) surface[30,31] and, in addition, showed a good agreement for the resulting surface electronic states.[32] We simulate the Ge(001) surface by means of repeated asymmetric slabs of eight Ge layers and a vacuum region of the same size. The top five Ge layers are allowed to relax and the bottom side of each slab (with fixed atomic positions) is saturated by H atoms in order to simulate the continuation of the Ge bulk.

We calculate the ground-state total energy for $c(8 \times 2)$ as well as $c(4 \times 2)$ coverages with 26 configurations in total. Structures are built for Au atoms on substitutional and adsorption sites. In each case, we find the lowest energy of the $c(4 \times 2)$ coverage at least 0.8 eV below that of the $c(8 \times 2)$ coverage. Subsequently, we thus focus on the $c(4 \times 2)$ coverage, for which we consider 11 configurations. Zero-point
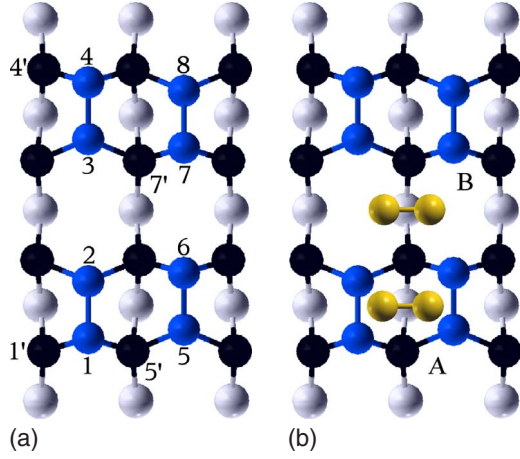
FIG. 1. (Color online) (a) Relaxed clean Ge(001) surface with the most likely Au positions for a coverage of 1/4 ML. Labels with tilde correspond to atoms in the second layer. (b) Adsorption sites of Au surface dimers. Ge surface atoms, second layer atoms, and third layer atoms are shown in blue (dark gray), black, and light gray, respectively.

energies are not included. We substitute two atoms of the Ge(001) surface by Au [see Fig. 1(a)] and account for the adsorbed Au dimers shown in Fig. 1(b). The surface formation energy per unit cell is given by

$$\Omega_f = E_{\text{Au/Ge(001)}} - \mu_{\text{Ge}} N_{\text{Ge}} - \mu_{\text{Au}} N_{\text{Au}} - \mu_{\text{H}} N_{\text{H}}, \quad (1)$$

where $E_{\text{Au/Ge(001)}}$ is the total energy of a slab containing N_{Ge} ($N_{\text{Au}}, N_{\text{H}}$) Ge (Au, H) atoms. The corresponding chemical potentials are represented by $\mu_{\text{Ge}}(\mu_{\text{Au}}, \mu_{\text{H}})$. Since Eq. (1) gives the formation energy of both surfaces of the slab, and we are only interested in the surface with the adsorbed Au atoms, we only study the relative formation energy of the Au-covered system

$$\Delta\Omega_f = E_{\text{Au/Ge(001)}} - E_{\text{Au/Ge(001)}}^{ref} - \mu_{\text{Ge}}(N_{\text{Ge}} - N_{\text{Ge}}^0), \quad (2)$$

with respect to a reference adsorbate $E_{\text{Au/Ge(001)}}^{ref}$.

The 13 configurations reported in this work are labeled according to their Au positions on the Ge(001) surface [see Figs. 1(a) and 1(b)]. The relative surface energies are calculated by Eq. (2) (see the summary in Table I, where the 2–8 model is the reference system). By the spin-orbit correction, the energies of the various configurations are modified and also new features appear in the electronic dispersion: shifts of energy levels, reflecting a spin-orbit splitting and "kinks" in the band structure, compare the later discussion. In the case of Au dimers, models A and B, the relaxation breaks up the Au-Au dimer bond and a single Au atom is adsorbed. In model A, each Au atom bonds to the nearest Ge dimer atom by breaking up the buckled dimer, while the next dimer row is not affected. However, in model B, the bond length of the 4 Ge surface dimers increases from 2.58 Å (see the top view in Fig. 2) to 2.68, 2.75, 2.87, and 2.66 Å.

The 1–6 and 2–5 models show a zig-zag order of Au-Ge dimers in a single row, while the next row is formed by Ge-Ge dimers. The relative surface energy difference is very small. A reason could be that in the 2–5 model, the Ge-Ge/

TABLE I. Relative surface formation energy as defined from Eq. (2), in meV/1×1 unit cell, for the Au/Ge(001) adsorbate system. Fixed Au number $N_{\text{Au}} = 2$ and H number $N_{\text{H}} = 16$, per asymmetric slab. The number of Ge atoms (N_{Ge}) varies. For $\Delta\Omega_f$, the 2–8 model is used as reference system. Values in brackets are obtained without spin-orbit interaction. Beyond, $\mu_{\text{Ge}} = -4.50$ eV, $\mu_{\text{Au}} = -3.60$ eV, and $\mu_{\text{H}} = -3.35$ eV.

Model	N_{Ge}	$\Delta\Omega_f$		Model	N_{Ge}	$\Delta\Omega_f$	
A	64	871	(839)	2–5	62	74	(81)
B	64	859	(816)	1–8	62	191	(211)
4′–7	62	595	(668)	2–8	62	0	(0)
1–5	62	20	(49)	1–7′	62	690	(764)
1–6	62	90	(96)	2–7′	62	459	(508)
1–7	62	382	(421)	2–4′	62	461	(511)
1′–5′	62	649	(751)				

Au-Ge dimers maintain the asymmetric order of the clean Ge(001) surface, as it is illustrated in Fig. 2. In contrast, in the 1–6 model, the asymmetric dimer order in the [110] direction is broken, while a zig-zag order along the [001] direction is maintained. The 1–7 model is very closely related to the experimental structure,[5] despite its $c(4 \times 2)$ coverage.
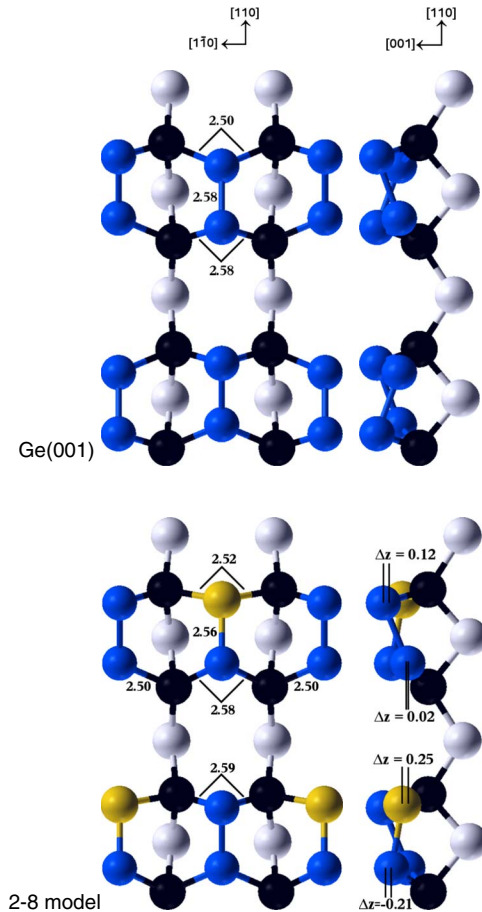
FIG. 2. (Color online) Top and side views of the relaxed clean Ge(001) surface and the 2–8 model. Δz denotes the shift of the dimer atoms with respect to the clean surface. All values are given in Å.
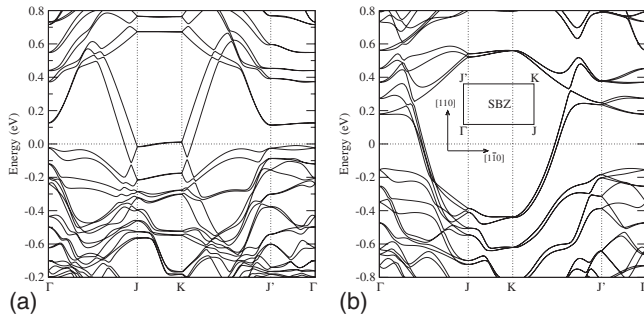
FIG. 3. Electronic band structures for the models (a) 1–5 and (b) 2–8. The zero energy is given by the Fermi level.

The Au atoms occupy upper dimer sites and are strongly bound to the second Ge layer and the lower Ge dimer atom. A structure optimization leads to an essentially flat surface similar to nonrelaxed Ge(001) with two dangling bonds. Thus, both the zig zag and the asymmetric order of the dimers disappear.

In the 1–8 model, the Au atoms occupy one upper and one lower dimer sites. The first Au atom breaks the asymmetric order of the buckled dimers (similar to 1–7), while the second does not affect the dimer (similar to 2–8). As a consequence, the 1–8 model lies, energetically, between the 1–7 and 2–8 models, in which the gold atoms have a larger distance to each other. The second lowest relative surface energy is found for the 1–5 model. Here, the Au atoms are arranged as chains running in $[1\bar{1}0]$ direction, alternately occupying upper and lower dimer sites. Each Au chain is separated from the next chain by almost 16 Å, which is exactly the reported experimental value. We observe that the Au-Ge dimers again form a flat surface, while the Ge-Ge dimers maintain the asymmetric order. The z coordinate of a Ge-Ge dimer's center of mass deviates from the respective value for an Au-Ge dimer by only 0.04 Å. Unlike the 1–7 and 1–8 models in which the horizontal dimer order increases the surface energy, here an increase is compensated by the Au-Au interaction.

The lowest-energy configuration is the 2–8 model, with a $c(4 \times 2)$ order, as seen in Fig. 1. In this case, the dimers are ordered asymmetrically, as in the clean Ge(001) surface. Our results show a tendency to preserve the bond distances of the Au-Ge dimer, both in the Ge-Ge dimers and on the second Ge layer. A comparison between the 2–8 model and the relaxed clean Ge(001) surface is shown in Fig. 2, including several dimer bond lengths. The values illustrate the modification due to the introduction of Au atoms. Δz quantifies the shifts of the dimer atoms with respect to the clean surface.

In order to identify the effects of the Au-Au bonding and the interplay with the Ge surface, we turn to the electronic band structure shown in Fig. 3 for the 1–5 and 2–8 models along selected high-symmetry lines of the surface Brillouin zone. The energy zero is defined by the Fermi level. Because the bands above 0.5 eV and below −0.5 eV mainly represent states of the clean Ge(001) surface, we focus on the energy range ±0.5 eV around the Fermi energy, which is influenced by the Au-Ge interplay. For the 1–5 model, the bands in this energy range resemble those of the tetradimer chain (TDC) model for the Pt/Ge(001) system.[33] In the TDC model, the Pt
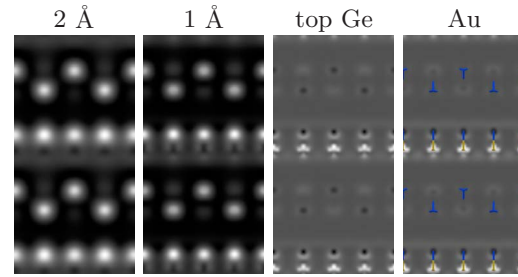
FIG. 4. (Color online) STM images of a 2×2 supercell simulated for the 1–5 model at −0.2 V. The constant-height images are calculated for planes 2, 1, and 0 Å above the topmost Ge atoms and at the Au atoms. Au panel: Ge and Au atoms are marked blue (dark gray) and yellow (light gray), respectively.

atoms likewise replace Ge dimer atoms, but there is another Ge-Ge dimer in the B position of Fig. 1(b), bound to the Pt atoms and the Ge atoms in the next dimer row.

According to Fig. 3, the bands around the Fermi level show large dispersions along $\Gamma - J$ and $K - J'$, i.e., along the Au chains in the $[1\bar{1}0]$ direction. On the other hand, there is
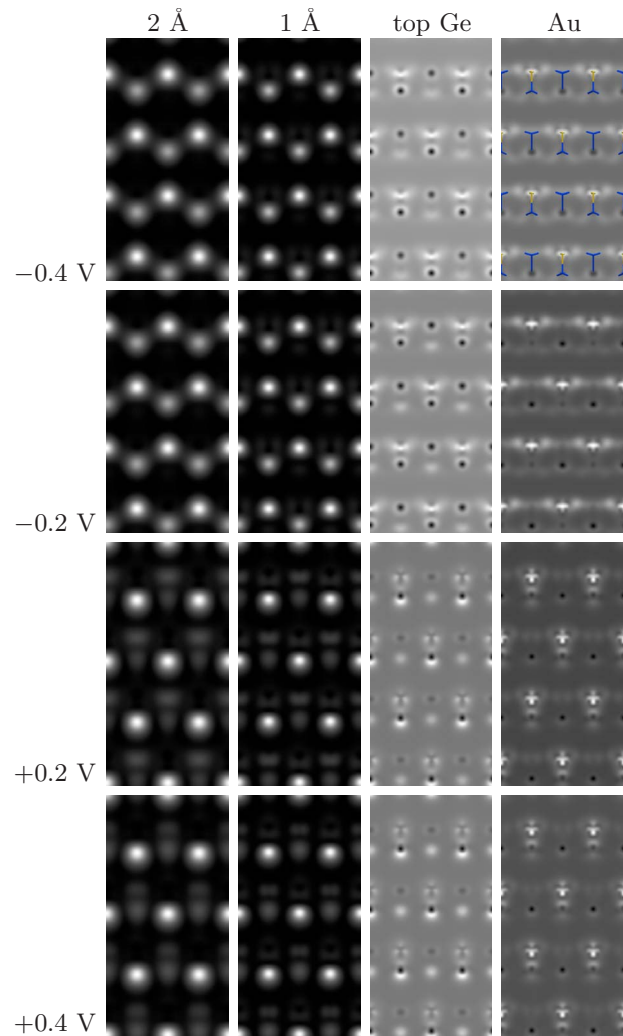
FIG. 5. (Color online) STM images of a 2×2 supercell simulated for the 2–8 model between −0.4 and +0.4 V, analogous to Fig. 4. Positive voltages refer to unoccupied states.

much less dispersion along $J-K$ and $J'-\Gamma$, i.e., perpendicular to the chains. By increasing the fineness of the k sampling, we have verified that the "kinks" visible in the band structures are no artifacts. A band crossing at these points definitely can be excluded by an analysis of the eigenvectors corresponding to the nearby bands.

Different dispersions along the high-symmetry lines of the Brillouin zone are confirmed by the STM images in Fig. 4. These constant-height images are calculated for a voltage of -0.2 V and planes 2, 1, and 0 Å above the topmost surface Ge atoms. Moreover, we study a plane just above the Au atoms. Figure 4 illustrates the formation of an Au chain in $[1\bar{1}0]$ direction. A pronounced dispersion dependence on the wire direction has also been obtained experimentally.[5]

The bands are more dispersive along $\Gamma-J$ and $K-J'$ for the 2–8 model, as compared to the 1–5 model, which is explained by the alignment of the Au atoms along the $[1\bar{1}0]$ direction. Because of the smaller distance between the Au atoms in the $[1\bar{1}0]$ than in the $[110]$ direction, the dispersive character of the bands is increased. The dispersion along $\Gamma-J$ strongly distinguishes the 2–8 model from the 1–5 model. The bands behave similar to those of the clean Ge(001) surface because the 2–8 model maintains the asymmetric dimers. In contrast, the 1–5 model has both a row of horizontal Au-Ge dimers in the $[1\bar{1}0]$ direction and a row of asymmetric Ge-Ge dimers. This fact is reflected by the simulated STM images for the 1–5 model in Fig. 4. We find a linear structure of horizontal Au-Ge dimers and a zig-zag structure of Ge-Ge dimers. For the 2–8 model, the simulated STM images in Fig. 5 show zig-zag chains, as known from

clean Ge(001). In the Au layer, we find in the occupied range $(-0.4$ V, -0.2 V) the (one dimensional) delocalized nanowire states. It has been pointed out in Ref. 5 that STM data are not able to clarify the atomic composition of the Au/Ge(001) surface due to atomic localization effects. According to our calculations, this fact is rather due to the reconstruction of the Au atoms on the surface. Because our data show that the metallic wires are formed below the topmost Ge layer, an observation by STM will be difficult.

To conclude, we have investigated the formation of Au chains on the reconstructed Ge(100) surface by means of density-functional theory. We show that it is important to include spin-orbit effects to properly describe the surface energies and the electronic structure. We also find a good agreement between our calculations and previously reported experiments. Our ground-state solutions reveal two competitive structures with a similar surface energy but different reconstruction patterns. In the first, the Au atoms sit on top of the Ge surface, whereas in the second they are located below the topmost Ge layer. STM simulations indicate that the Au chains can be detected only in a very narrow voltage range. Our results demonstrate that they are almost perfectly one dimensional with very little dispersion in the perpendicular direction.

*udo.schwingenschlogl@kaust.edu.sa
[1] N. Nilius, T. M. Wallis, and W. Ho, Science **297**, 1853 (2002).
[2] J. Lagoute, X. Liu, and S. Fölsch, Phys. Rev. B **74**, 125410 (2006).
[3] A. I. Yanson *et al.*, Nature (London) **395**, 783 (1998).
[4] S. R. Bahn and K. W. Jacobsen, Phys. Rev. Lett. **87**, 266101 (2001).
[5] J. Schäfer, C. Blumenstein, S. Meyer, M. Wisniewski, and R. Claessen, Phys. Rev. Lett. **101**, 236802 (2008).
[6] S. Tomonaga, Prog. Theor. Phys. **5**, 544 (1950).
[7] J. M. Luttinger, J. Math. Phys. **4**, 1154 (1963).
[8] F. D. M. Haldane, Phys. Rev. Lett. **47**, 1840 (1981).
[9] I. G. Hill and A. B. McLean, Phys. Rev. B **56**, 15725 (1997).
[10] J. R. Ahn, P. G. Kang, K. D. Ryang, and H. W. Yeom, Phys. Rev. Lett. **95**, 196402 (2005).
[11] J. Wang, M. Li, and E. I. Altman, Phys. Rev. B **70**, 233312 (2004); Surf. Sci. **596**, 126 (2005).
[12] A. van Houselt, M. Fischer, B. Poelsema, and H. J. W. Zandvliet, Phys. Rev. B **78**, 233410 (2008).
[13] R. Koch *et al.*, Appl. Phys. A: Mater. Sci. Process. **55**, 417 (1992).
[14] J. J. Schulz, M. Sturmat, and R. Koch, Phys. Rev. B **62**, 15402 (2000).
[15] O. Gurlu *et al.*, Appl. Phys. Lett. **83**, 4610 (2003).
[16] N. Oncel, A. van Houselt, J. Huijben, A. S. Hallback, O. Gurlu, H. J. W. Zandvliet, and B. Poelsema, Phys. Rev. Lett. **95**, 116801 (2005).

[17] U. Schwingenschlögl and C. Schuster, EPL **81**, 26001 (2008); Eur. Phys. J. B **60**, 409 (2007).
[18] A. A. Stekolnikov, F. Bechstedt, M. Wisniewski, J. Schafer, and R. Claessen, Phys. Rev. Lett. **100**, 196101 (2008).
[19] P. Hohenberg and W. Kohn, Phys. Rev. **136**, B864 (1964); W. Kohn and L. J. Sham, Phys. Rev. **140**, A1133 (1965).
[20] H. Kim and J. R. Chelikowsky, Phys. Rev. Lett. **77**, 1063 (1996).
[21] P. E. Blöchl, Phys. Rev. B **50**, 17953 (1994).
[22] G. Kresse and D. Joubert, Phys. Rev. B **59**, 1758 (1999).
[23] G. Kresse and J. Hafner, Phys. Rev. B **47**, 558 (1993); **49**, 14251 (1994).
[24] G. Kresse and J. Furthmüller, Comput. Mater. Sci. **6**, 15 (1996); Phys. Rev. B **54**, 11169 (1996).
[25] J. P. Perdew, K. Burke, and M. Ernzerhof, Phys. Rev. Lett. **77**, 3865 (1996); **78**, 1396 (1997).
[26] P. Pyykko, Angew. Chem., Int. Ed. **43**, 4412 (2004); A. Castro *et al.*, J. Chem. Phys. **129**, 144110 (2008).
[27] H. J. Monkhorst and J. D. Pack, Phys. Rev. B **13**, 5188 (1976).
[28] P. Krüger and J. Pollmann, Phys. Rev. Lett. **74**, 1155 (1995).
[29] H. J. W. Zandvliet, Phys. Rep. **388**, 1 (2003).
[30] S. Ferrer *et al.*, Phys. Rev. Lett. **75**, 1771 (1995).
[31] Y. Yoshimoto *et al.*, Phys. Rev. B **61**, 1965 (2000).
[32] U. Schwingenschlögl and C. Schuster, Chem. Phys. Lett. **449**, 126 (2007).
[33] A. A. Stekolnikov, J. Furthmüller, and F. Bechstedt, Phys. Rev. B **78**, 155434 (2008).